Received: 2 June 2020 | Revised: 10 August 2020 | Accepted: 13 August 2020

DOI: 10.1111/cas.14625

ORIGINAL ARTICLE

Cancer Science WILEY

PSMB8 inhibition decreases tumor angiogenesis in glioblastoma through vascular endothelial growth factor A reduction

Hsin-Han Chang[1,2] | Yu-Chen Cheng[1,2] | Wen-Chiuan Tsai[3] | Ying Chen[1,2]

[1]Department of Biology and Anatomy, National Defense Medical Center, Taipei, Taiwan

[2]Graduate Institute of Life Science, National Defense Medical Center, Taipei, Taiwan

[3]Department of Pathology, Tri-Service General Hospital, National Defense Medical Center, Taipei, Taiwan

Correspondence
Ying Chen, Department of Biology and Anatomy, National Defense Medical Center, Neihu District, Taipei, Taiwan.
Email: ychen0523@mail.ndmctsgh.edu.tw

Wen-Chiuan Tsai, Department of Pathology, Tri-Service General Hospital, National Defense Medical Center, Taipei, Taiwan.
Email: ab95057@hotmail.com

Funding information
Ministry of Science and Technology, Taiwan, Grant/Award Number: MOST-107-2320-B-016-011-MY3; Ministry of National Defense-Medical Affairs Bureau, Grant/Award Number: MAB-109-065

Abstract

Glioblastoma, also known as glioblastoma multiforme (GBM), is a fast-growing tumor and the most aggressive brain malignancy. Proteasome subunit beta type-8 (PSMB8) is one of the 17 essential subunits for the complete assembly of the 20S proteasome complex. The aim of the present study was to evaluate the role of PSMB8 expression in GBM progression and angiogenesis. PSMB8 expression in glioblastoma LN229 and U87MG was knocked down by siRNA or inducible shRNA both in vitro and in vivo. After PSMB8 reduction, cell survival, migration, invasion, angiogenesis, and the related signaling cascades were evaluated. An orthotopic mouse tumor model was also provided to examine the angiogenesis within tumors. A GEO profile analysis indicated that high expression of PSMB8 mRNA in GBM patients was correlated with a low survival rate. In immunohistochemistry analysis, PSMB8 expression was higher in high-grade than in low-grade brain tumors. The proliferation, migration, and angiogenesis of human GBM cells were decreased by PSMB8 knockdown in vitro. Furthermore, phosphorylated focal adhesion kinase (p-FAK), p-paxillin, MMP2, MMP9, and cathepsin B were significantly reduced in LN229 cells. Integrin β1 and β3 were reduced in HUVEC after incubation with LN229-conditioned medium. In an orthotopic mouse tumor model, inducible knockdown of PSMB8 reduced the expression of vascular endothelial growth factor (VEGF), VEGF receptor, and CD31 as well as the progression of human glioblastoma. In this article, we demonstrated the role of PSMB8 in glioblastoma progression, especially neovascularization in vitro and in vivo. These results may provide a target for the anti–angiogenic effect of PSMB8 in glioblastoma therapy in the future.

KEYWORDS

angiogenesis, endothelial cell, glioblastoma, PSMB8

Wen-Chiuan Tsai and Ying Chen contributed equally to this research.

1 | INTRODUCTION

1.1 | Glioblastoma multiforme

Glioblastoma multiforme (GBM) is the most aggressive, invasive, and undifferentiated type of brain tumor and has been classified as grade IV by the World Health Organization (WHO).[1] Unlike other solid tumors, glioblastoma widely invades the surrounding brain but rarely metastasizes.[2] Even if the patient receives standard radiotherapy combined with temozolomide (TMZ), the overall 5-year survival rate is 9.8%, and approximately 75% of high-grade glioblastoma patients die within the first year after diagnosis.[3] The growth of glioblastoma is supported by angiogenesis and tumor vasculature, supplying oxygen and nutrients and modulating the immune response.[4,5] Glioblastoma releases proangiogenic factors that promote the development of tumor vasculature, including transforming growth factor β, vascular endothelial growth factor (VEGF), nitric oxide, proteolytic enzymes, ribonucleases, and chemokines.[4,5] In the tumor microenvironment (TME), endothelial cells (EC) rely on active communication between stromal and tumor cells, soluble factors, and extracellular matrix (ECM). Vascular endothelial growth factor A induces the formation of motile EC to break down the surrounding ECM and to develop new vascular sprouts.[5] Therefore, inhibiting angiogenesis might block tumor progression.

1.2 | PSMB8

Proteasome subunit beta type-8 (PSMB8; or large multifunctional peptidase 7 [LMP7]) is a member of the 20S proteasome.[6] The 20S proteasome contains seven α-type structural subunits acting as gate structures and seven β-type structures that form the proteolytic domain.[6,7] PSMB8 is a member of the immunoproteasome, which is induced by IFN-γ or TNF-α.[6] The immunoproteasome has higher chymotrypsin-like activity than the standard proteasome.[6,8,9] A previous study showed that chymotrypsin-like and trypsin-like activities are increased in the immunoproteasome to produce antigenic peptides that bind to major histocompatibility complex class I molecules.[6] Inducing immunoproteasome expression leads to cell metabolism, differentiation, and immune regulation.[6] PSMB8 overexpression correlates with gastric cancer progression, especially aspects related to the depth of tumor invasion and lymph node metastasis.[10] In glioblastoma, PSMB8 inhibition induces apoptosis and blocks migration and invasion via PI3K/AKT regulation.[11] However, whether PSMB8 regulates angiogenesis and the underlying mechanisms in GBM remain unclear.

2 | MATERIALS AND METHODS

2.1 | Analysis of human glioma datasets from the GEO database

Genomic data sets from the NCBI GEO database were analyzed. Briefly, PSMB8 mRNA expression, age, pathologic grading of primary glioma, and overall survival time were obtained from the GDS1815:202243_s_at database. Seventy-seven datasets were used in the statistical analyses.

2.2 | Immunohistochemical staining of human glioma specimens

A glioma tissue microarray (GL807a; Biomax) was incubated with a rabbit anti–human PSMB8 monoclonal antibody (Abcam) at room temperature. Information on the antibodies is presented in Table S1. After 16 hours of incubation, the samples were incubated with biotin-labeled secondary immunoglobulin and treated with 3-amino-9-ethylcarbazole substrate chromogen (DAKO, Glostrup, Denmark) to visualize peroxidase activity.

2.3 | Cell culture

The human glioblastoma cell lines LN229 and U87MG were obtained from the ATCC. LN229-Luc2 cells were derived from a stable transfection of pLuc2-iRFP and selected using a BD FACSAria sorter (BD Biosciences). LN229-Luc2 cells were stably transfected with shRNA against PSMB8 and selected by puromycin. The cells were grown in RPMI-1640 containing 10% FBS (Life Technologies) in a humidified atmosphere of 5% CO2 at 37°C. HUVEC were purchased from the Bioresource Collection and Research Center in Taiwan and cultured in endothelial cell media (ScienCell Research Laboratories).

2.4 | Drugs

Doxycycline hyclate, MTT, sucrose, and DMSO were obtained from Sigma-Aldrich. Neutral buffered formalin (10%) was purchased from Leica Biosystems. TMZ was purchased from MedChem Express.

2.5 | Antibodies

For western blotting and immunohistochemistry (IHC) staining, rabbit anti–PSMB8, GAPDH, p65, and FAK were purchased from Cell Signaling Technology. Moreover, rabbit anti–VEGFR and anti–CD31 were purchased from Abcam. Mouse anti–VEGFA was purchased from Santa Cruz. Mouse anti–phospho-STAT3, p-FAK, p-paxillin, paxillin, MMP2, MMP9, and Cathepsin B were purchased from BD. Information on the antibodies is shown in Table S1.

2.6 | siRNA transfection

LN229 and U87MG glioblastoma cells were transfected with 50 nM predesigned PSMB8 siRNA and control siRNA (Ambion) with the

RNAiMAX Lipofectamine reagent (Life Technologies). The sequences of siRNA targeting PSMB8 are shown in Table S2. After 24 h of transfection, the culture medium was replaced with DMEM containing 10% FBS before subsequent experiments.

2.7 | Plasmid construction

The lentiviral vectors pAS4.1w.Ppuro-aOn, pCMV-dR8.91, pAS1w.8xTetO, and pMD2.G were provided by the National RNAi Core Facility at Academia Sinica in Taiwan. The shRNA sequence was cloned into pAS1w.8xTetO according to the RNAi Core lab protocol. The sequences of the shRNA are showed in Table S3. The PSMB8 cDNA was cloned into pAS4.1w.Ppuro-aOn vector by Kpn I and NheI.

2.8 | Cell survival assay

LN229 and U87MG glioblastoma cells were cultured in a 24-well plate. Different siRNA or a vehicle control were then transfected into GBM cells for 24, 48, and 72 hours. After the cells were washed with PBS (137 mM NaCl, 2.7 mM KCl, 1.5 mM KH2PO4, 8 mM Na2HPO4, and pH 7.4), 0.5 mg/mL MTT was added and incubation was continued for another 3 h. The cells were then lysed with DMSO. The absorbance at 590 nm was measured.

2.9 | Cell migration assay

Cell migration was assayed via wound healing and Transwell assays. LN229 glioblastoma cells were seeding in a 6-well plate to form a monolayer. After being scratched with a P200 pipette tip and imaged, the cells were then cultured for 16 h. The wound area was analyzed by ImageJ. The Transwell migration assay was performed by seeding 4×10^4 LN229 glioblastoma cells and 2×10^4 HUVEC in the upper chamber of a Transwell insert (Corning Costar). After incubation at 37°C for 16 h, the cells on the lower side were fixed with 10% formalin in PBS and stained with Coomassie Brilliant Blue G250 (Sigma). The migrated cells were examined in three randomly selected fields from each membrane in five independent experiments.

2.10 | Cell invasion assay

The Transwell invasion assay was performed by seeding 4×10^4 LN229 glioblastoma cells in the upper chamber of a Transwell insert. Before cell seeding, 0.5% Matrigel in a coating buffer solution (BD) was added to the upper chamber. The cells on the lower side were fixed and stained. The invaded cells were counted in three randomly selected fields from each membrane in five independent experiments.

2.11 | Tube formation assay

Matrigel (50 mL/well) was added to a precooled 96-well plate and incubated for 1 hour at 37°C. HUVEC (1×10^4) were seeded into each well with 50% conditioned medium (CM). After 6 hours of incubation, tube formation was imaged. Then, angiogenesis was quantified and analyzed by ImageJ.

2.12 | Real-time PCR analysis

The extracted RNA was reverse-transcribed to cDNA with a PrimeScript RT reagent kit (Takara Bio). The LightCycler 480 Instrument II (Roche Life Science) Real-Time PCR System was used to quantify mRNA with the SensiFAST SYBR No ROX Kit (Bioline) according to the protocol provided by the manufacturer. The oligonucleotide primers used were as follows: PSMB8, 5′-ACTGGTTATGGTGCATACTTG/TTGTAAGAACGGGCATCTC-3′, VEGFA, 5′ -AGGGCAGAATCATCACGAAGT/AGGGTCTCGATTGGATGGCA-3′ and GAPDH, 5′-AGCCACATCGCTCAGACACC/GTACTCAGAGGCCAGCATCG-3′. The GAPDH gene was used as an endogenous control.

2.13 | Western blotting

After various treatments, glioblastoma cells were homogenized in protein extraction buffer (GE Healthcare Life Sciences) with proteinase inhibitor and phosphatase inhibitor (MedChem Express). Protein samples were electrophoresed on a 10% SDS-PAGE and then transferred to a nitrocellulose membrane (Bio-Rad). Strips from the membrane were blocked with 5% nonfat milk in Tris-buffered saline, pH 7.4, containing 0.1% Tween (TBS-Tween). Then, the membranes were incubated with primary antibodies in blocking solution overnight at 4°C. After being washed, the strips were incubated with a 1:5000 or 1:10 000 dilution of HRP-conjugated anti–rabbit or anti–mouse IgG antibody from Cell Signaling Technology. Next, the blots were reacted with the ECL substrate developing solution (Bio-Rad). The density of the bands on the nitrocellulose membrane (Bio-Rad) was captured and quantified by densitometry analysis using ImageJ. The density of the control sample was 100%, and the density of the test sample was relative to the density of the internal control.

2.14 | Orthotopic xenograft animal model

All mouse experiments were approved by the laboratory animal center of the National Defense Medical Center, Taiwan (IACUC No. 17-119). BALB/c AnN.Cg-*Foxnl*^{nu}/CrlNarl (female, 8-week-old) mice were provided by the National Laboratory Animal

Center, NARLabs, Taiwan. The mice were killed with 12.5 mg/kg tiletamine-zolazepam (Zoletil 50, Virbac) and 5 mg/kg xylazine (Rompun). Next, 1×10^5 LN229 cells with inducible knockdown by an shRNA to PSMB8 or a scramble control were implanted into the right cerebral hemisphere of the mice. Five days after implantation, the mice were assigned to four groups that received vehicle control, TMZ, shPSMB8, or shPSMB8 + TMZ treatments (n = 5 for each group). TMZ was administered via oral gavage at 5 mg/kg for 7 days. To induce knockdown, 2 mg/mL doxycycline in drinking water with 0.1% sucrose was administered after implantation. The body weights of the mice were measured three times per week. The implanted tumors were monitored with a noninvasive In Vivo Imaging System (IVIS) (PerkinElmer) three times per week, and the bioluminescence intensity was compared after mice were intraperitoneally injected with D-luciferin firefly and potassium salt (Biosynth, Swiss) in PBS. After 12 days, mice were killed with tiletamine-zolazepam and xylazine, and the brains were fixed in formalin, embedded in paraffin, and cut into serial sections.

2.15 | Histological and immunohistochemical examination

Brain tissues were excised, rinsed twice in PBS, and fixed in 10% formaldehyde. Tissues were frozen and sliced into 5-μm-thick sections. Routine H&E staining was performed to facilitate histological evaluation. Protein expression in the brain tumors of the nude mice was detected by IHC staining. Protein primary antibodies and secondary goat anti–rabbit antibodies (Jackson ImmunoResearch Laboratories) were used. The expression of protein was observed in 10 random fields for each group.

2.16 | ELISA for vascular endothelial growth factor A in condition medium

Concentrations of VEGFA were measured using commercially available ELISA (R&D System) according to the guidelines of the manufacturer. The values obtained after ELISA were corrected with a dilution factor and finally expressed in nanograms per milliliter.

2.17 | Statistical analysis

The overall survival datasets (GDS1815/202243_s_at/PSMB8) obtained from the GEO database were analyzed using the Kaplan-Meier method. A single-tailed test was used to calculate the *PSMB8* expression level in the groups of WHO pathologic grade gliomas. The cohorts of low versus high *PSMB8* gene expression were estimated for both WHO grade III and grade IV human glioma groups. The cutoff value of *PSMB8* expression was based on the conditional inference tree generated by the "party" package with R language (R 3.1.2 software). All experiments were performed at least three times, and the results are expressed as the means ± SEM for the total number of experiments. Differences between means were assessed using the Kruskal-Wallis test. The Mann-Whitney test was used for a post hoc analysis. Statistical significance was set at $P < 0.05$.

3 | RESULTS

3.1 | PSMB8 was correlated with the survival rate of glioblastoma multiforme patients

The expression of PSMB8 was elevated in tumor tissue (Figure 1A and B). PSMB8 mRNA expression profiles in patients with different grades of glioma were analyzed (data accessible at the NCBI GEO database, accession GSE 16 011, and GDS1962/1555852). Moreover, analysis of PSMB8 expression was performed for a tissue array of glioma tissues including nonneoplastic brain tissue, pilocytic astrocytoma, diffuse astrocytoma, anaplastic astrocytoma, and GBM (Figure 1C). PSMB8 immunostaining in low-grade (grade I and II) glioma was nearly 30.4-fold higher than that in nonneoplastic brain tissues. In high-grade (grade III and IV) glioma, the average PSMB8 immunostaining scores were 162.5-fold higher than those in nonneoplastic brain tissues (Figure 1D). Therefore, these results revealed the association of PSMB8 with advanced grades of glioma.

3.2 | PSMB8 inhibition decreased the survival rate in human glioblastoma cell lines

Compared to that in human astrocytes, PSMB8 expression was higher in the glioblastoma cell lines LN229, U87MG, and GBM8401 (Figure 2A). When PSMB8 expression was inhibited by siRNA transfection for 24, 48, and 72 hours, PSMB8 expression in LN229 cell was reduced to 85%, 35%, and 17%. PSMB8 expression in U87MG cells was reduced to 76%, 42%, and 20% at 24, 48, and 72 hours, respectively. Moreover, the LN229 cell survival rate was reduced to 81%, 77%, and 61.3% at 24, 48, and 72 hours, respectively. The U87MG cell survival rate was reduced to 73.9%, 74.3%, and 58.9% at 24, 48, and 72 hours, respectively (Figure 2B and C). While PSMB8 overexpression was induced in LN229 cells by the Tet-On system, the cell survival rate was not significantly changed compared to the control group (Fig. S1B).When PSMB8 was knocked down in combination with 100, 200, and 300 μM TMZ for 72 h, the survival rate was reduced to 44.9%, 30.5%, and 20.7%, respectively, in LN229 cells. The survival rate was significantly reduced to 54.9%, 45.7%, and 33.7% after treatment with 100, 200, and 300 μM TMZ alone, respectively, in LN229 cells. When PSMB8 was knocked down in combination with 100, 200, and 300 μM TMZ for 72 h, the survival rate was reduced to 46.5%, 38.9%, and 23.8%, respectively, in U87MG cells. The survival

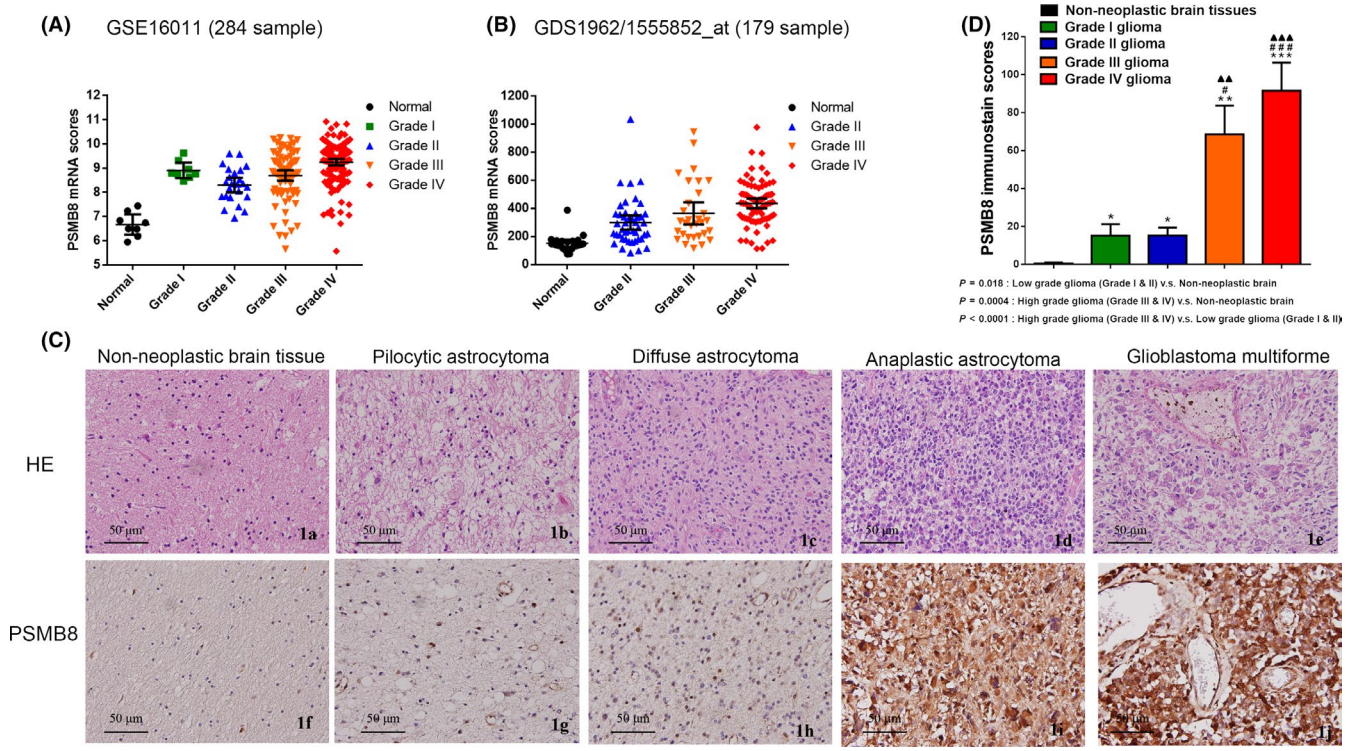

FIGURE 1 PSMB8 was correlated with survival in glioblastoma multiforme (GBM) patients. (A) and (B) PSMB8 mRNA expression profiles in different grade glioblastoma patients (data accessible at the NCBI GEO database, accession GSE 16 011, and GDS1962/1555852). (C) H&E staining of nonneoplastic brain tissue 1a, pilocytic astrocytoma 1b, diffuse astrocytoma 1c, anaplastic astrocytoma 1d, and glioblastoma multiforme 1e and immunohistochemical analysis of PSMB8 in nonneoplastic brain tissue (1f), pilocytic astrocytoma 1g, diffuse astrocytoma 1h, anaplastic astrocytoma 1i, and glioblastoma multiforme 1j. (Original magnification: ×400) (D) Quantification of 1a-1j

rate was significantly reduced to 53.2%, 47.8%, and 36.1% after treatment with 100, 200, and 300 μM TMZ alone, respectively, in U87MG cells. (Figure 2D). These results demonstrated that the decreased PSMB8 expression reduced the survival rate and tolerance to TMZ in both LN229 and U87MG cells.

3.3 | Migration and invasion were decreased by PSMB8 knockdown in LN229 *cells*

Following transfection with siRNA for 16 h, the cell migration was reduced significantly compared to that of the control group in the wound healing assay (Figure 3A). In the Transwell assay, the migration rate was reduced to 72.5% compared to that of the control groups. The invasion ability was reduced to 77.5% relative to that of the control groups (Figure 3B). While PSMB8 overexpression was induced in LN229 cells by the Tet-On system, the migration and invasion ability of LN229 were unaffected compared to the control groups (Supplementary Fig. S1D).

The expression of focal adhesion-related and invasion-related proteins was analyzed after siPSMB8 transfection in LN229 cells for 24 and 48 hours. It was interesting that p-FAK, p-paxillin, MMP2, MMP9, and cathepsin B levels were significantly reduced after siPSMB8 transfection for 24 hours. After 48 hours of transfection of siPSMB8, integrin β1 and β3 were decreased, which may impair adhesion ability in glioblastoma cells (Figure 3C). These results suggested that the migration and invasion abilities were decreased by PSMB8 knockdown with the reduction of focal adhesion complex and invasion-related proteins in glioblastoma cells.

3.4 | Tubulogenesis of endothelial cells was reduced by knockdown of PSMB8 in glioblastoma cells

To further investigate the interaction between glioblastoma and endothelial cells, tetracycline-induced shPSMB8 glioblastoma cell lines were established by lentivirus infection. After doxycycline was induced for 48 and 96 hours, PSMB8 expression was reduced 40% and 60%, respectively compared to the scramble control group in LN229 cells (Figure 4A). Wound healing migration assay showed that the migration ability of HUVEC was unaffected compared to that of the control group in the conditioned medium collected from shPSMB8 LN229 cells (Figure 4B). The endothelial network formation of HUVEC was decreased after treatment with glioblastoma-conditioned medium. In addition, analysis of the endothelial network indicated that total length, segment length, and branch points were reduced to 80% compared to those of the control group. The cell junctions were reduced 90% compared to those in the control groups (Figure 4D). When HUVEC treated with conditioned medium from the inducible PSMB8 overexpressed

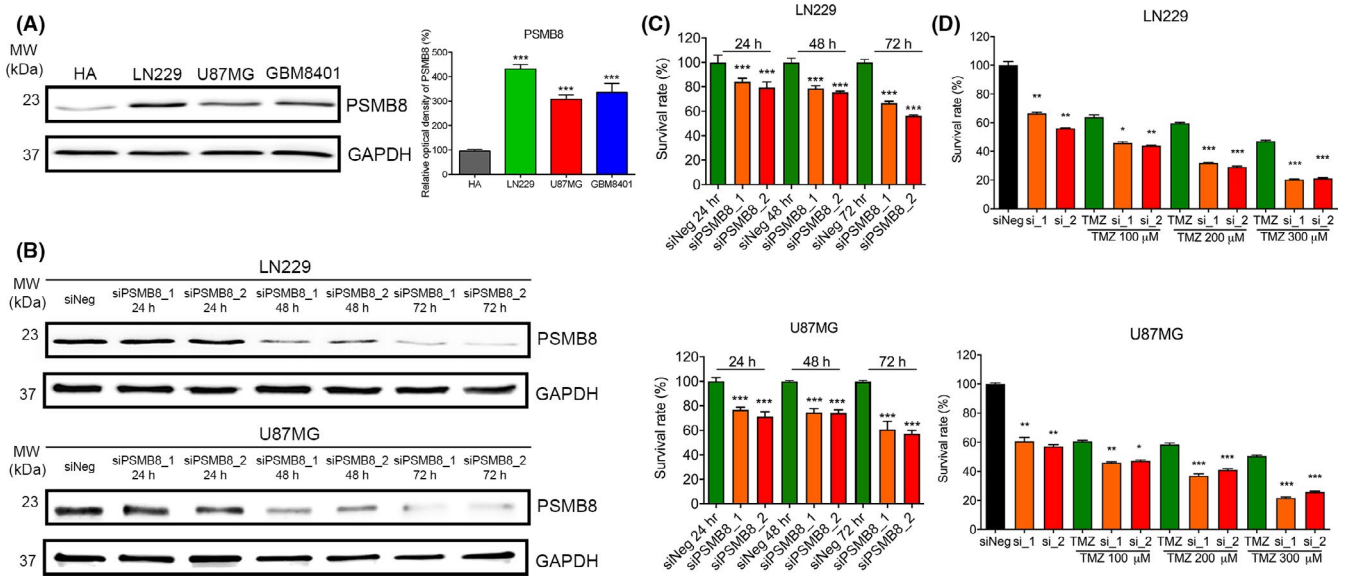

FIGURE 2 Inhibiting PSMB8 expression decreased the survival rate of glioblastoma cell lines. (A) The PSMB8 expression level was analyzed in different glioblastoma cell lines. HA, human astrocyte. The right panels show the quantitative analyses (n = 3). (B) PSMB8 protein expression in LN229 and U87MG cells was downregulated after siRNA treatment for 24, 48, and 72 h (n = 3). (C) The cell survival rate of glioblastoma cell lines was downregulated after siRNA treatment for 24, 48, and 72 h, as demonstrated by MTT assay (n = 6). (D) The cell survival rate of glioblastoma cell lines was downregulated by the combined treatment of siRNA and temozolomide (TMZ) (n = 6). $^{*}P < 0.05$; $^{**}P < 0.01$; $^{***}P < 0.001$ compared with the control group

LN229 cells, this showed no difference in the angiogenetic ability in HUVEC (Fig. S1E).These results suggested that the angiogenesis of endothelial cells was inhibited by PSMB8 knockdown in glioblastoma cells.

3.5 | Inducible knockdown of PSMB8 inhibited vascular endothelial growth factor A expression in LN229 cells and integrin expression in HUVEC

Because angiogenesis of endothelial cells was blocked by PSMB8 inhibition in glioblastoma cells, the angiogenetic related proteins were further examined. As expected, VEGFA protein expression was significantly reduced to 88% compared to the scramble control group in LN229 cells. The mRNA expression of VEGFA was not affected after PSMB8 inhibition (Fig. S2A). The VEGFA concentration was also reduced from 350 pg/mL to 250 pg/mL after tetracycline-induced knockdown for 48 hours in LN229 conditioned medium (Fig. S2B). Moreover, the p-Stat3, HIF1-α, and COX2 protein expression levels were increased by PSMB8 knockdown in LN229 cells (Figure 5A). When endothelial cells were treated with LN229 conditioned medium, the expression of integrin β1 and β3 was reduced to 63% and 65%, respectively. In contrast, p-FAK/FAK and p-paxillin/paxillin protein expressions were not affected by PSMB8 inhibition (Figure 5B). These results indicated that the reduced angiogenetic ability of HUVEC might be due to the inhibition of VEGFA in LN229 cells and integrin in HUVEC. In contrast, the expressions of p-ERK, ERK, and VEGFA in HUVEC had no significant difference compared to the control group after being treated with condition medium from knockdown PMSB8 LN229 cells (Supplementary Fig. S3).

3.6 | Inducible knockdown of PSMB8 inhibited tumor progression in an orthotropic human glioblastoma xenograft mouse model

LN229 cells expressing tetracycline-induced shPSMB8 were implanted into nude mice to evaluate the role of PSMB8 in glioblastoma in vivo. After inducing shPSMB8 for 12 days, the total luminescence was significantly reduced 50% compared to that in the scramble control group. Knockdown of PSMB8 combined with TMZ treatment was more effective in tumor progression than TMZ alone (Figure 6A and B). VEGFA and VEGFR expression was reduced in the TMZ, shPSMB8, and TMZ + shPSMB8 groups (Figure 6C). The vessels within the tumor were reduced in the TMZ + shPSMB8 group,

FIGURE 3 Migration and invasion were decreased with PSMB8 knockdown. (A) Wound healing migration assays in LN229 cells after 0 and 16 h of siRNA treatment. The right panels show the quantitative analyses of the wound healing rate compared to the control group rate (n = 5). (B) Transwell migration assays in LN229 cells after 16 h of siRNA treatment. The right panels show the quantitative analyses of the Transwell migration rate compared to the control group rate (n = 6). (C) The expression of focal adhesion-related and invasion-related proteins was downregulated by siRNA treatment in LN229 cells after 16 h (n = 6). The plotted graph shows the protein quantitative analysis results. $^{*}P < 0.05$; $^{**}P < 0.01$; $^{***}P < 0.001$ compared with the control group (n = 5)

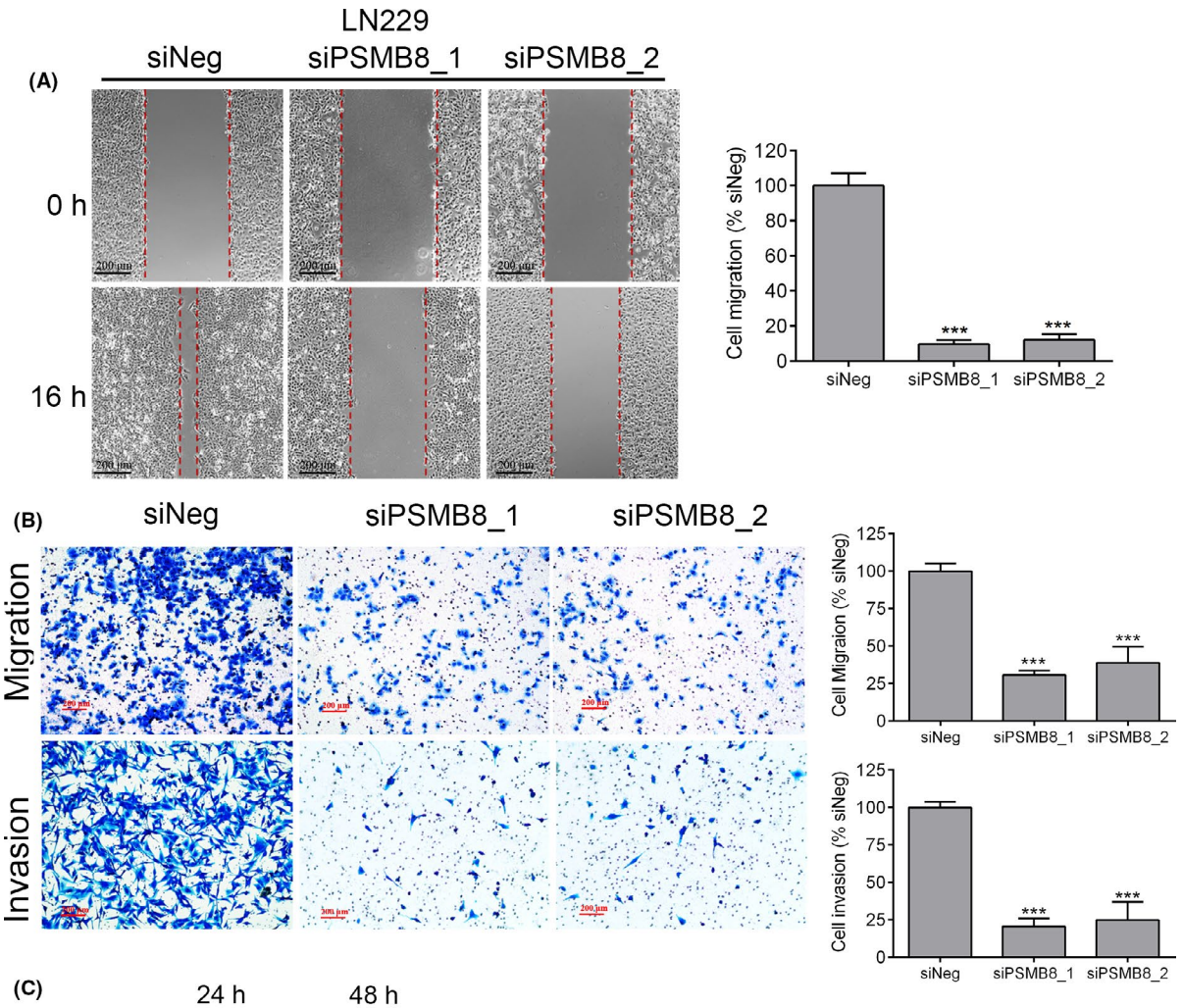
LN229
siNeg
siPSMB8_1
siPSMB8_2
(A)
0 h
16 h
200 μm
Cell migration (% siNeg)
120
100
80
60
40
20
0
***
***
siNeg
siPSMB8_1
siPSMB8_2
(B)
siNeg
siPSMB8_1
siPSMB8_2
Migration
Invasion
Cell Migraion (% siNeg)
125
100
75
50
25
0
***
***
Cell invasion (% siNeg)
125
100
75
50
25
0
***
***
siNeg
siPSMB8_1
siPSMB8_2

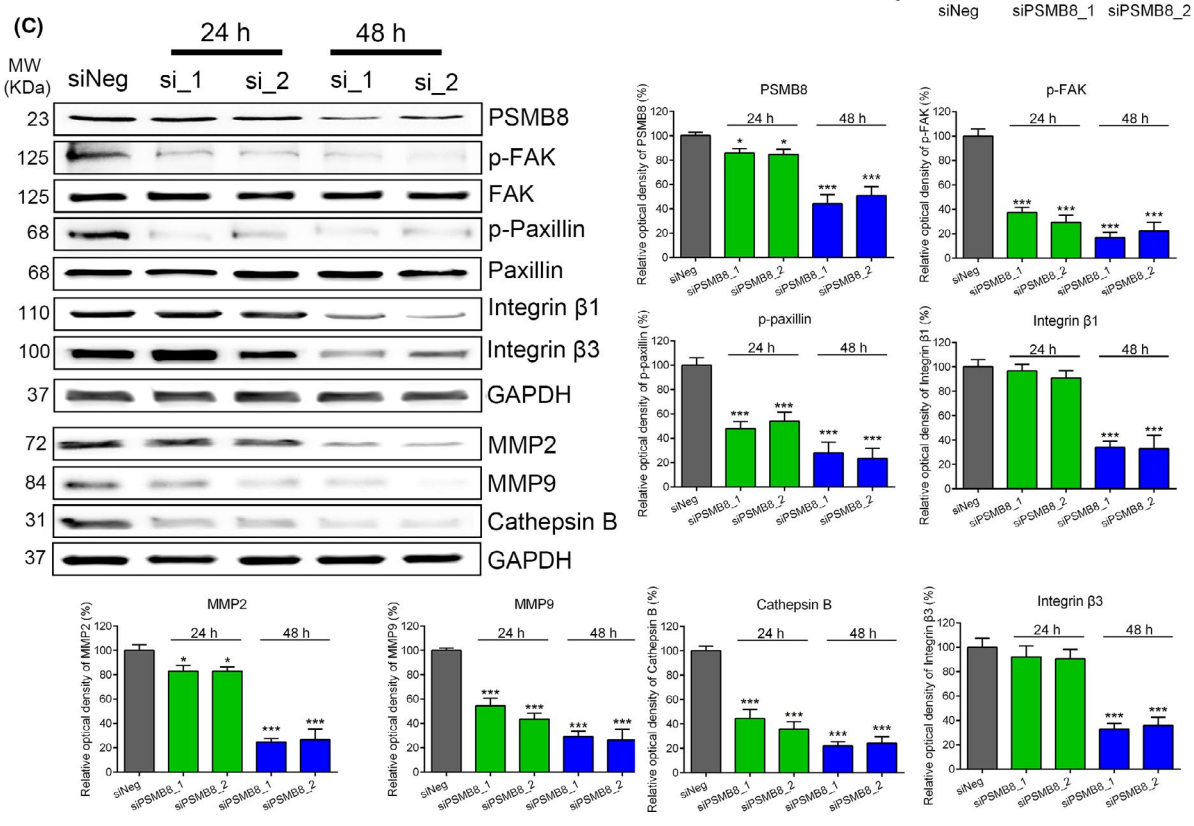
(C)
24 h
48 h
MW (KDa)
siNeg
si_1
si_2
si_1
si_2
23
PSMB8
125
p-FAK
125
FAK
68
p-Paxillin
68
Paxillin
110
Integrin β1
100
Integrin β3
37
GAPDH
72
MMP2
84
MMP9
31
Cathepsin B
37
GAPDH
PSMB8
p-FAK
p-paxillin
Integrin β1
MMP2
MMP9
Cathepsin B
Integrin β3
Relative optical density of PSMB8 (%)
Relative optical density of p-FAK (%)
Relative optical density of p-paxillin (%)
Relative optical density of Integrin β1 (%)
Relative optical density of MMP2 (%)
Relative optical density of MMP9 (%)
Relative optical density of Cathepsin B (%)
Relative optical density of Integrin β3 (%)
24 h
48 h
siNeg
siPSMB8_1
siPSMB8_2

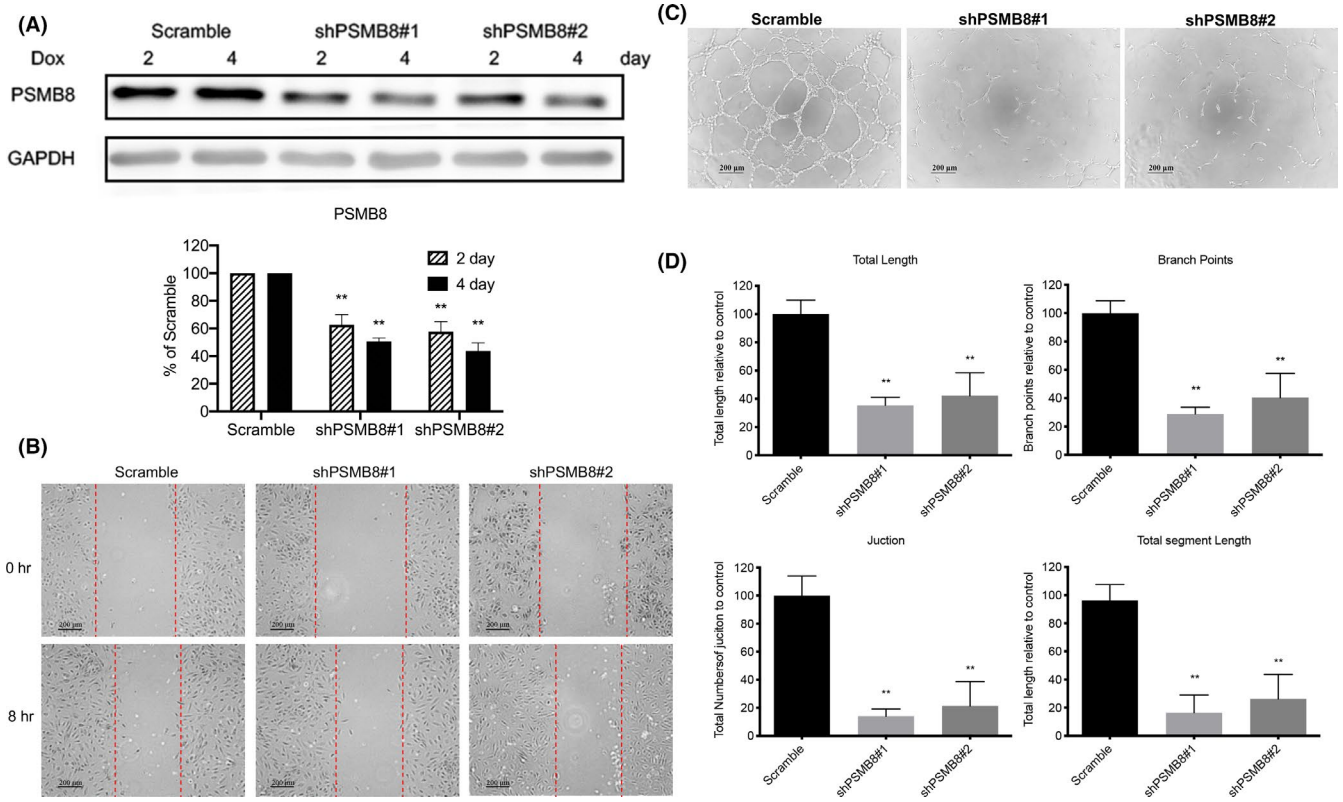

FIGURE 4 Migration ability and tubulogenesis of endothelial cells were reduced by knockdown of PSMB8 in glioblastoma cells. (A) PSMB8 protein was downregulated by doxycycline-induced shPSMB8 in LN229 cells. The lower panels showed the quantitative analyses (n = 5). (B) Wound healing assay of HUVEC treated with conditioned medium from shPSMB8#1 and shPSMB8#2 LN229 cells for 8 h (n = 10). (C) Endothelial network formation in HUVEC treated with conditioned medium from shPSMB8#1 and shPSMB8#2 LN229 cells for 6 h (n = 6). (D) Quantification of the length of capillary-like structure, number of branch points, and number of junctions. $^{*}P < 0.05$; $^{**}P < 0.01$ compared with the control group

which was demonstrated by H&E and CD31 staining (Figure 6C). These data suggested that the knockdown of PSMB8 reduced tumor progression in LN229 cells in vivo with a reduction in VEGFA and VEGFR expression.

4 | DISCUSSION

Temozolomide treatment combined with PSMB8 knockdown reduced the survival rate of LN229 and U87MG glioblastoma cells in vitro. TMZ is the first-line chemotherapeutic drug for GBM treatment, but the human glioblastoma cell line LN229 is resistant to TMZ.[6,12,13] IFN-β increases sensitivity to TMZ and has been shown to improve the therapeutic outcome in GBM patients.[14] In our previous study, the knockdown of PSMB4 expression enhanced the antitumor effect of TMZ on tumor growth in an orthotropic GBM xenograft mouse model.[13] In this study, knockdown of PSMB8 expression enhanced the antitumor effect of TMZ on tumor growth not only in vitro but also in vivo. PSMB4 is a crucial subunit that supports the formation of the 20S proteasome complex.[13] Unlike PSMB4, PSMB8 is induced by IFNγ and TNF to replace PSMB5.[12,15-17] PSMB8 is a 20S proteasome subunit with stronger chymotrypsin-like ability to cleave hydrophobic residues than PSMB5.[6,15,17] TMZ combined with knockdown of PSMB8 is suggested as a therapeutic treatment for human glioblastoma.

The reduction in PSMB8 inhibited the migration and invasion of LN229 cells. The PSMB8 3′UTR has been reported to be a target of miR-451. Overexpression of miR-451 suppresses PSMB8, NOS2, VEGF, MMP-2, and MMP-9, which may suppress the growth and migration of the lung cancer cell line A549.[18] In addition, PSMB8 reduces migration, proliferation, and apoptosis through the ERK1/2 and PI3K/AKT signaling pathways in U87MG cells.[11] In our previous study, knockdown of PSMB4 expression reduced the levels of integrin β1, β3, p-FAK, MMP2, and MMP9 in LN229 cells. The phosphorylation of FAK and paxillin catalyzes downstream signals, including Rac, ERK, and PI3K, leading to cell proliferation, cytoskeleton assembly, and cell invasion.[13] Here, the phosphorylation of FAK and paxillin and the expression of MMP2, MMP9, and cathepsin B were also inhibited by knockdown of PSMB8 in LN229 cells. Therefore, PSMB8 inhibition in glioblastoma cells blocked glioblastoma cell migration and invasion through cathepsin B activation and the integrin/FAK/paxillin pathways.

Tumor cells contain various angiogenic factors, including VEGF, neuropilins, and integrins, which initiate chemical stimulation during the angiogenesis process.[19] Several studies have shown that VEGFA-mediated angiogenesis is the leading factor for the

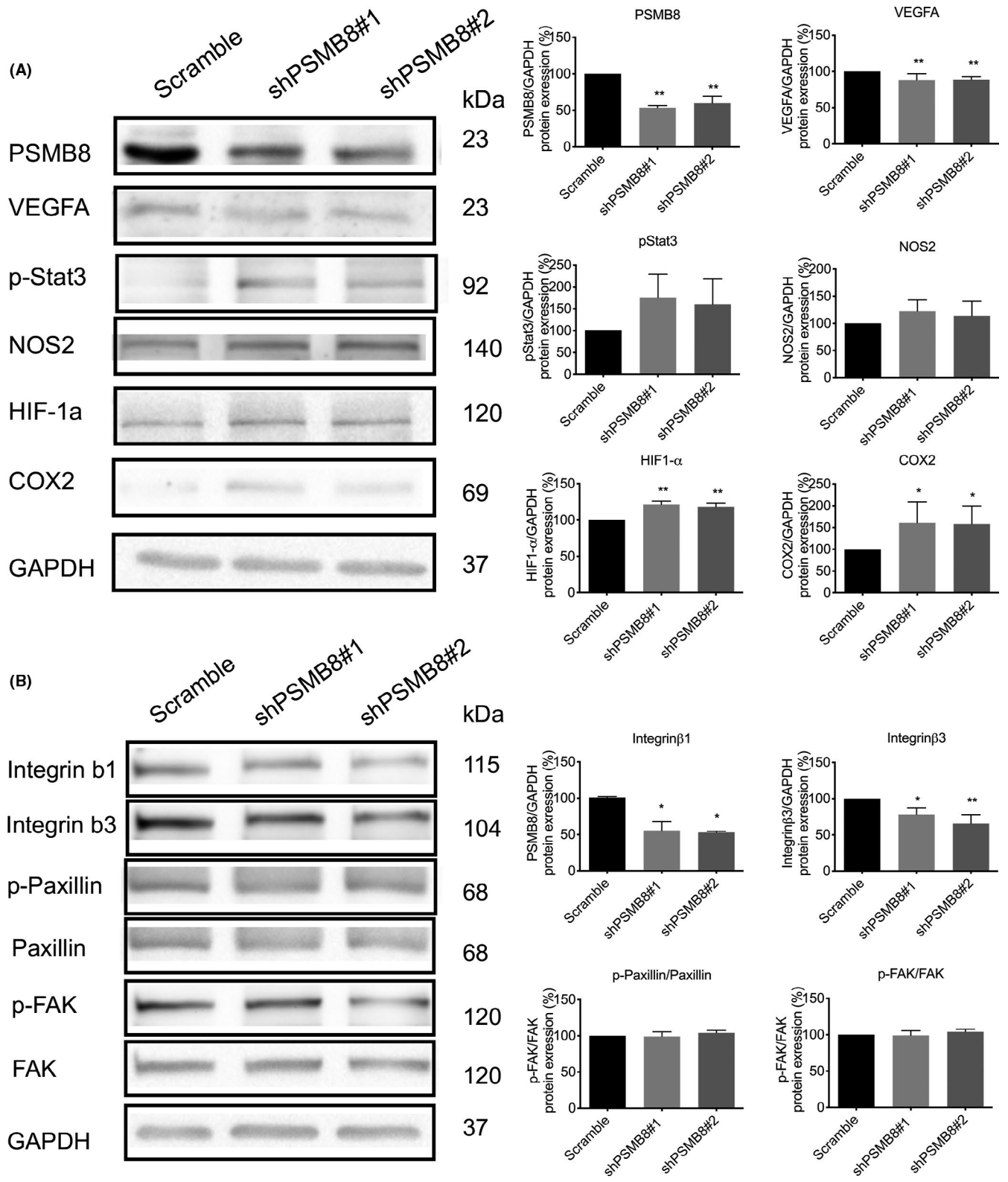

FIGURE 5 Focal adhesion protein expression in endothelial cells was reduced by knockdown of PSMB8 in glioblastoma cells. (A) PSMB8, VEGFA, phosphorylated Stat3, NOS2, HIF1-α, and COX2 expression in LN229 cells. The right panels show the quantitative analyses (n = 5). (B) Integrin β1, integrin β3, phosphorylated paxillin, paxillin, phosphorylated FAK, and FAK expression in HUVEC treated with conditioned medium for 6 h. The right panels show the quantitative analyses (n = 5). $^{*}P < 0.05$; $^{**}P < 0.01$ compared with the control group

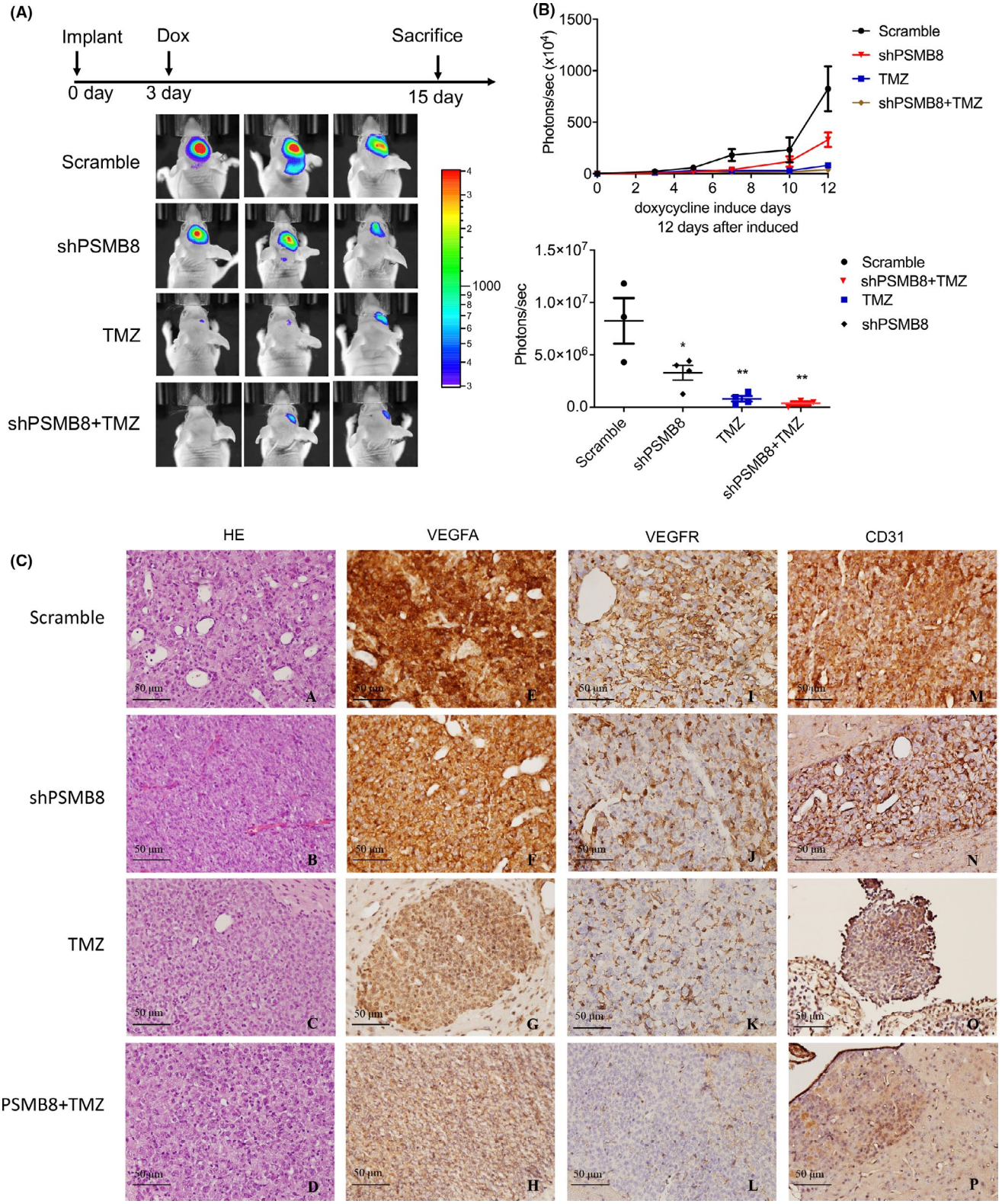

FIGURE 6 Induced expression shRNA to PSMB8 in LN229 cells reduced tumor progression in an orthotropic human glioblastoma xenograft mouse model. (A) The in vivo bioluminescent imaging data of different groups were analyzed via the In Vivo Imaging System (IVIS) system. (B) Knockdown of PSMB8 in glioblastoma reduced tumor progression. (C) Representative image of histological staining of xenograft orthotropic brains. H&E staining of the scramble (A), shPSMB8 (B), temozolomide (TMZ) (C), and shPSMB8 + TMZ (D) groups. Immunohistochemistry (IHC) analysis of vascular endothelial growth factor A (VEGFA) in the scramble (E), shPSMB8 (F), TMZ (G), and shPSMB8 + TMZ (H) groups. IHC analysis of vascular endothelial growth factor receptor 2 (VEGFR2) in the scramble (I), shPSMB8 (J), TMZ (K), and shPSMB8 + TMZ (L) groups. IHC analysis of CD31 in the scramble (M), shPSMB8 (N), TMZ (O), and shPSMB8 + TMZ (P) groups. Original magnification: ×400. V = vessel (n = 5)

progression of breast cancer, lung cancer, and glioblastoma, providing essential nutrients for increased growth and tumor progression.[5,20-22] The expression of integrin β1 in endothelial cell is essential for angiogenesis.[23] VEGF can interact with integrin by VEGFR2 and activate the binding function of multiple integrins in both endothelial and tumor cells through the PI3K/AKT pathway.[24] Impairing the interaction between integrin α2β1 and VEGFR2 inhibits angiogenesis and migration of HUVEC.[25] Here, we examined whether the impaired angiogenesis may correlate with integrin and VEGF downregulation.

It has been reported that hypoxia dramatically increases with tumor grade in astrocytic tumors.[26] IL-1β-mediated NF-kB activation by the PI3K-AKT-mTOR pathway induces an increase in HIF-1α in a COX-2-dependent manner and induces VEGF expression in A549 cells.[18] In lung cancer, PSMB8 is correlated with NOS2 to suppress the growth and migration of lung cancer.[18] In our study, knockdown of PSMB8 expression in glioblastoma cells interfered with VEGFA expression and angiogenesis in HUVEC; however, HIF-1α, COX2, and NOS2 protein expression increased in LN229 cells. The reduction of VEGFA in LN229 cells may be regulated through other signaling pathways, which needs further investigation. Therefore, PSMB8 played an essential role in the expression of VEGFA and other proangiogenic factors in a manner independent of HIF-1α and NOS2.

Our results demonstrated the significance of PSMB8 depletion in glioblastoma angiogenesis and its association with reduced VEGFA protein production but not VEGFA transcription. VEGFA is a common downstream target of p53, c-jun, and c-Fos in malignancies.[27-29] Comparatively, our results showed increased PSMB8 expression in GBM tissues, and the pathogenic roles of p53, c-jun, and c-Fos are well characterized in brain tumor research.[30-32] In addition, reduced PSMB8 expression impairs VEGFA protein stability, which is affected by ubiquitination and degradation in a PKA-dependent and Smad3-dependent and Smad2-independent pathway in colon cancer.[33] A similar phenomenon is also reported with ubiquitination protein accumulation in PSMB8 inhibited JASL (Japanese auto-inflammatory syndrome with lipodystrophy) cells.[34] Moreover, PSMB8 inhibition accumulates the polyubiquitinated proteins in THP-1 cells.[35] Here, the regulation of VEGFA may not be directly through the proteolysis of glioma PSMB8.

Targeting the immunoproteasome system with bortezomib has shed light on the treatment of hematologic malignancies.[36] However, previous pharmacokinetic studies indicated limited distribution of bortezomib in the central nervous system that impeded its application in brain tumor therapy.[37] Reduced tumor burden in a PSMB8-knockdown GBM xenograft model served as the rationale for a PSMB8-based inhibitor for future brain tumor management. In addition, anti–angiogenic therapy with bevacizumab has been approved for GBM management with unmet needs in tumor resistance.[38,39] Our results showed the potency of PSMB8 inhibition in GBM angiogenesis, adding value of drug designation by targeting PSMB8. Future PSMB8 research in GBM could not only demonstrate its potential as a second-generation proteasome inhibitor but reinforce its synergetic effects with current anti–angiogenesis agents.

5 | CONCLUSION

The migration ability of HUVEC was not affected by knockdown PSMB8 in glioblastoma cells. Integrin β3 plays a critical role in pathological angiogenesis.[40,41] β3-endonexin is a binding partner for the integrin β3 and is able to enhance HUVEC tube formation but is not required for VEGF-induced HUVEC adhesion and migration.[41] In the present study, the integrin β3 in HUVEC was significantly reduced by LN229 conditioned medium. Based on these results, knockdown of PSMB8 in glioblastoma cells inhibited angiogenesis in HUVEC may be a result of the reduction of integrin β3.

ACKNOWLEDGEMENTS

We appreciate the technical assistance and animal care provided by the Instrument Center and Animal Center in the National Defense Medical Center, Taiwan. We Also thank the National RNAi Core Facility in Academia Sinica in Taiwan for providing shRNA reagents and related services. This research was supported by grants from the Ministry of Science and Technology (MOST-107-2320-B-016-011-MY3) and the Ministry of National Defense-Medical Affairs Bureau (MAB-109-065).

CONFLICT OF INTEREST

The authors declare that they have no conflict of interest.

.

ORCID

Hsin-Han Chang https://orcid.org/0000-0002-5824-7079
Ying Chen https://orcid.org/0000-0001-6303-5858

REFERENCES

1. Hanif F, Muzaffar K, Perveen K, Malhi SM, Simjee SU. Glioblastoma multiforme: a review of its epidemiology and pathogenesis through clinical presentation and treatment. *Asian Pac J Cancer Prev*. 2017;2017:3-9.
2. Lathia JD, Mack SC, Mulkearns-Hubert EE, Valentim CLL, Rich JN. Cancer stem cells in glioblastoma. *Genes Dev*. 2015;29:1203-1217.
3. Stupp R, Hegi ME, Mason WP, et al. Effects of radiotherapy with concomitant and adjuvant temozolomide versus radiotherapy alone on survival in glioblastoma in a randomised phase III study: 5-year analysis of the EORTC-NCIC trial. *The Lancet Oncology*. 2009;10:459-466. http://dx.doi.org/10.1016/s1470-2045(09)70025-7.
4. Broekman ML, Maas SLN, Abels ER, Mempel TR, Krichevsky AM, Breakefield XO. Multidimensional communication in the microenvirons of glioblastoma. *Nature Reviews Neurology*. 2018;14:482-495. http://dx.doi.org/10.1038/s41582-018-0025-8.
5. De Palma M, Biziato D, Petrova TV. Microenvironmental regulation of tumour angiogenesis. *Nat Rev Cancer*. 2017;2017:457-474.
6. Kimura H, Caturegli P, Takahashi M, Suzuki K. New insights into the function of the immunoproteasome in immune and nonimmune cells. *J Immunol Res*. 2015;2015:1-8.
7. Murata S, Yashiroda H, Tanaka K. Molecular mechanisms of proteasome assembly. *Nat Rev Mol Cell Biol*. 2009;2009:104-115.

8. Tanaka K. The proteasome: from basic mechanisms to emerging roles. *Keio J Med*. 2013;62:1-12.
9. Britton M, Lucas MM, Downey SL, et al. Selective inhibitor of proteasome's caspase-like sites sensitizes cells to specific inhibition of chymotrypsin-like sites. *Chem Biol*. 2009;16:1278-1289.
10. Kwon CH, Park HJ, Choi YR, et al. PSMB8 and PBK as potential gastric cancer subtype-specific biomarkers associated with prognosis. *Oncotarget*. 2016;7:21454-21468.
11. Yang B-Y, Song J-W, Sun H-Z, et al. PSMB8 regulates glioma cell migration, proliferation, and apoptosis through modulating ERK1/2 and PI3K/AKT signaling pathways. *Biomed Pharmacother*. 2018;100:205-212.
12. Kimura H, Usui F, Karasawa T, et al. Immunoproteasome subunit LMP7 deficiency improves obesity and metabolic disorders. *Sci Rep*. 2015;2015:15883.
13. Cheng Y-C, Tsai W-C, Sung Y-C, Chang H-H, Chen Y. Interference with PSMB4 expression exerts an anti–tumor effect by decreasing the invasion and proliferation of human glioblastoma cells. *Cell Physiol Biochem*. 2018;45:819-831.
14. Volak A, LeRoy SG, Natasan JS, et al. Virus vector-mediated genetic modification of brain tumor stromal cells after intravenous delivery. *Journal of Neuro-Oncology*. 2018;139:293-305. http://dx.doi.org/10.1007/s11060-018-2889-2.
15. Groettrup M, Kirk CJ, Basler M. Proteasomes in immune cells: More than peptide producers? *Nat Rev Immunol*. 2010;10:73-78.
16. Ferrington DA, Immunoproteasomes GDS. structure, function, and antigen presentation. *Prog Mol Biol Transl Sci*. 2012;2012:75-112.
17. Rousseau A, Bertolotti A. Regulation of proteasome assembly and activity in health and disease. *Nature Reviews Molecular Cell Biology*. 2018;19:697-712. http://dx.doi.org/10.1038/s41580-018-0040-z.
18. Yin P, Peng R, Peng H, et al. MiR-451 suppresses cell proliferation and metastasis in A549 lung cancer cells. *Mol Biotechnol*. 2014;2015:1-11.
19. Nishida N, Yano H, Nishida T, Kamura T, Kojiro M. Angiogenesis in cancer. *Vasc Health Risk Manag*. 2006;2:213.
20. Marrogi AJ, Travis WD, Welsh JA, et al. Nitric oxide synthase, cyclooxygenase 2, and vascular endothelial growth factor in the angiogenesis of non-small cell lung carcinoma. *Clin Cancer Res*. 2000;6:4739-4744.
21. Treps L, Perret R, Edmond S, Ricard D, Gavard J. Glioblastoma stem-like cells secrete the pro-angiogenic VEGF-A factor in extracellular vesicles. *J Extra Ves*. 2017;6:1359479.
22. Saxena S, Jha S. Role of NOD- like Receptors in Glioma Angiogenesis: Insights into future therapeutic interventions. *Cytokine Growth Factor Rev*. 2017;2017:15-26.
23. Tanigawa K, Maekawa M, Kiyoi T, et al. SNX9 determines the surface levels of integrin β1 in vascular endothelial cells: Implication in poor prognosis of human colorectal cancers overexpressing SNX9. *J Cell Physiol*. 2019;234:17280-17294.
24. Parveen A, Subedi L, Kim HW, et al. Phytochemicals targeting VEGF and VEGF-related multifactors as anticancer therapy. *J Clin Med*. 2019;8:350.
25. Dos Santos PK, Altei WF, Danilucci TM, et al. Alternagin-C (ALT-C), a disintegrin-like protein, attenuates alpha2beta1 integrin and VEGF receptor 2 signaling resulting in angiogenesis inhibition. *Biochimie*. 2020;174:144-158.
26. Guadagno E, Presta I, Maisano D, et al. Role of Macrophages in Brain Tumor Growth and Progression. *International Journal of Molecular Sciences*. 2018;19:1005. http://dx.doi.org/10.3390/ijms19041005.
27. Ghahremani MF, Goossens S, Nittner D, et al. p53 promotes VEGF expression and angiogenesis in the absence of an intact p21-Rb pathway. *Cell Death Differ*. 2013;20:888-897.
28. Schmidt D, Textor B, Pein OT, et al. Critical role for NF-κB-induced JunB in VEGF regulation and tumor angiogenesis. *The EMBO J*. 2007;26:710-719.
29. Morfoisse F, Renaud E, Hantelys F, Prats A-C, Garmy-Susini B. Role of hypoxia and vascular endothelial growth factors in lymphangiogenesis. *Mol Cell Oncol*. 2015;2:e1024821.
30. Liu Z-G, Jiang G, Tang J, et al. c-Fos over-expression promotes radioresistance and predicts poor prognosis in malignant glioma. *Oncotarget*. 2016;7:65946.
31. Blau L, Knirsh R, Ben-Dror I, et al. Aberrant expression of c-Jun in glioblastoma by internal ribosome entry site (IRES)-mediated translational activation. *Proc Natl Acad Sci USA*. 2012;109:E2875-E2884.
32. Zhang Y, Dube C, Gibert M, et al. The p53 pathway in glioblastoma. *Cancers*. 2018;10:297.
33. Geng L, Chaudhuri A, Talmon G, Wisecarver JL, Wang J. TGF-Beta suppresses VEGFA-mediated angiogenesis in colon cancer metastasis. *PLoS One*. 2013;8:e59918.
34. Kitamura A, Maekawa Y, Uehara H, et al. A mutation in the immunoproteasome subunit PSMB8 causes autoinflammation and lipodystrophy in humans. *J Clin Investig*. 2011;121:4150-4160.
35. Rouette A, Trofimov A, Haberl D, et al. Expression of immunoproteasome genes is regulated by cell-intrinsic and–extrinsic factors in human cancers. *Sci Rep*. 2016;6:1-14.
36. Miller Z, Ao L, Bo Kim K, Lee W. Inhibitors of the immunoproteasome: current status and future directions. *Curr Pharm Des*. 2013;19:4140-4151.
37. Hemeryck A, Geerts R, Monbaliu J, et al. Tissue distribution and depletion kinetics of bortezomib and bortezomib-related radioactivity in male rats after single and repeated intravenous injection of 14C-bortezomib. *Cancer Chemotherapy and Pharmacology*. 2007;60:777-787. http://dx.doi.org/10.1007/s00280-007-0424-9.
38. Wenger KJ, Wagner M, You SJ, et al. Bevacizumab as a last-line treatment for glioblastoma following failure of radiotherapy, temozolomide and lomustine. *Oncol Lett*. 2017;14:1141-1146.
39. Li Y, Ali S, Clarke J, Cha S. Bevacizumab in recurrent glioma: patterns of treatment failure and implications. *Brain Tumor Res Treatment*. 2017;5:1-9.
40. Mahabeleshwar GH, Feng W, Phillips DR, Byzova TV. Integrin signaling is critical for pathological angiogenesis. *J Exp Med*. 2006;203:2495-2507.
41. Cao Z, Suo X, Chu Y, et al. Peptides derived from the integrin β cytoplasmic tails inhibit angiogenesis. *Cell Commun Signal*. 2018;16:1-15.

SUPPORTING INFORMATION

Additional supporting information may be found online in the Supporting Information section.

How to cite this article: Chang H-H, Cheng Y-C, Tsai W-C, Chen Y. PSMB8 inhibition decreases tumor angiogenesis in glioblastoma through vascular endothelial growth factor A reduction. *Cancer Sci*. 2020;111:4142–4153. https://doi.org/10.1111/cas.14625